IEEE Access
Multidisciplinary | Rapid Review | Open Access Journal

Received June 22, 2019, accepted June 30, 2019, date of publication July 10, 2019, date of current version July 29, 2019.

Digital Object Identifier 10.1109/ACCESS.2019.2927762

Time Domain Synchronous Moving Average and its Application to Gear Fault Detection

LUN ZHANG AND NIAOQING HU

Laboratory of Science and Technology on Integrated Logistics Support, National University of Defense Technology, Changsha 410073, China
College of Intelligence Science and Technology, National University of Defense Technology, Changsha 410073, China

Corresponding author: Niaoqing Hu (hnq@nudt.edu.cn)

This work was supported in part by the National Key Research and Development Program of China under Grant 2018YFB1702401, in part by the Defense Industrial Technology Development Program under Grant WDZC20195500305, and in part by the National Natural Science Foundation of China under Grant 51475463 and Grant 51775550.

ABSTRACT Periodic signal detection methods are widely used in applications including human detection and machinery fault diagnosis. Averaging is one of the most powerful filtering techniques for periodic signals extraction. Time domain synchronous average (TSA) and moving average (MA) are the most commonly used average techniques in engineering. TSA has the advantage at periodic signal detection by depressing noises and asynchronous signal components. MA is effective to remove noises while keeping signal periodicity. However, the TSA signal is not periodic as a measurement signal, and signal spectrum resolution degrades seriously; meanwhile, the MA filters out high-frequency signal components of interests. Detection of periodic signal among noises while keeping signal periodicity and high-frequency signal components become a challenge. To address this problem, time-synchronous moving average (TSMA) method is proposed as an improvement on TSA inspired by MA in this paper. Influences of signal overlap and properties of TSMA are investigated. Furthermore, a practical average times optimization method is given for reference. The correctness of theoretical deviations and effectiveness of the proposed method on periodic signal detection are validated using numerical simulations. At last, the proposed method is validated by an application on fault detection of the gearbox.

INDEX TERMS Signal processing, periodic signal detection, fault detection, gearbox.

I. INTRODUCTION

Periodic signal is one of the most general signal type including ECG(Electrocardiograph)[1], communication signals[2] and seismic signal[3]. In mechanical systems, spring-mass-damper system oscillates periodically after excitation. Rotary machineries like gears and bearings vibrate periodically during operation[4]–[6]. Reciprocating machinery like internal combustion engine[7] vibrates periodically as well.

Periodic signal detection is useful technique in many areas. Li et al. [8] studied through-wall human movement detection taking advantage of human periodic motion such as breathing and limb movement. Masatoshi [9] investigated non-contact heart rate detection method using periodic variations in doppler radar. Hyun Choi[10] proposed a high-speed periodic signal acquisition technique using incoherent sub-sampling and back-end signal reconstruction algorithms. Leeb et al. [11] developed a single-photon technique for the detection of periodic extraterrestrial laser pulses. Tsai and Perng [12] presented a technique for the inspection of defects in a two-dimensional periodic image using a multi-band-pass filter. Xu et al. [13] proposed a feature named envelop harmonic-to-noise ratio(EHNR) for periodic impulses detection, an EHNR-based method to locate the periodic impulses in frequency domain was applicated to bearing diagnosis. Yao and Ma [14] investigated the weak periodic signal detection by sine-Wiener-noise-induced resonance in the FitsHugh-Nagumo neuron. Yilmaz and Ozer [15] studied the effect of the delayed feedback loop on the weak periodic signal detection performance of a stochastic Hodgkin-Huxley neuron.

Among periodic signal detection techniques, averaging is one of the most powerful filtering techniques. McFadden and Smith [16] proposed a signal processing technique for gear local fault detection from average of the vibration signal. Then, the technique was applied to condition monitoring of rolling element bearings[17] and planetary gearboxes[18] as well. Leclère and Hamzaoui [19] analyzed

The associate editor coordinating the review of this manuscript and approving it for publication was Prakasam Periasamy.

fuzzy cyclostationary signals using the moving synchronous average. Guo et al. [20] proposed an envelope synchronous average scheme for multi-axis gear fault detection. Eric[21] investigated the performance of 6 time synchronous average algorithms. Ahamed et al. [22] used time synchronous average to detect spur gear tooth root crack under fluctuating speed. Inaki [23] applied dual-level time synchronous averaging on motor current signature analysis for condition monitoring of gearbox. Combet and Gelman [24] proposed an automated method for performing time synchronous averaging without speed sensor. Jong [25] proposed an autocorrelation-based time synchronous averaging method for condition monitoring of planetary gearboxes in wind turbines. Zhu et al. [26] combined synchronous averaging scanning on STFT(Short Time Fourier Transform) to detect the periodically occurring high -frequency transient under complicated conditions. Qin et al. [27] used time domain averaging approach to denoise the initial transient dictionary within his research on the transient feature extraction method by the improved orthogonal matching pursuit and K-SVD algorithm.

It is not difficult to find that TSA[28] and MA[29] are most usually used average techniques in engineering.

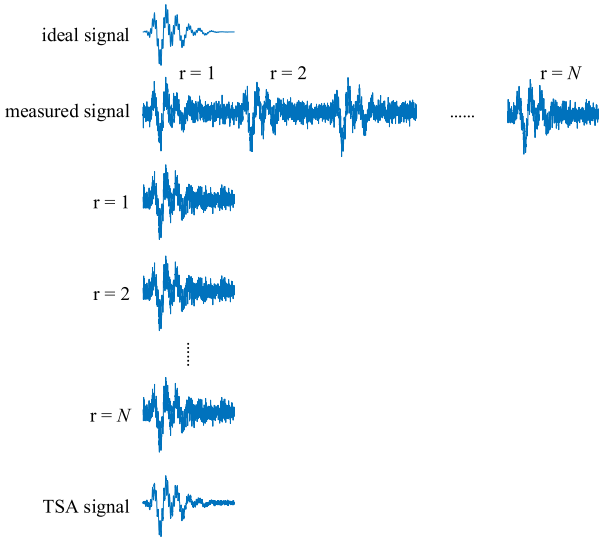

FIGURE 1. Illustration of TSA algorithm.

TSA (Time-domain Synchronous Average) is a popular technique that often used to process gear and bearing signals to detect potential fault of gearboxes. An intuitive implementation of TSA is shown in Figure 1. After measuring the signal N cycles, data segments of each cycle are firstly divided into each individual cycle, then data points in all data segments are averaged to generate TSA signal. Any periodical signal components that synchronous with this period stay unchanged after averaging, while other signals including asynchronous signals and noise will be attenuated towards zero. TSA is good at depressing noises and asynchronous signal components. It has been proved effective to detect periodic signal among noises in practice. But, as shown in Figure 1, TSA signal is no longer periodic since it averages signal samples from the beginning to the end. Only one cycle of the periodic signal will be covered in TSA signal. In addition, resolution of order spectrum degrades seriously from $1/N$ to 1[30].

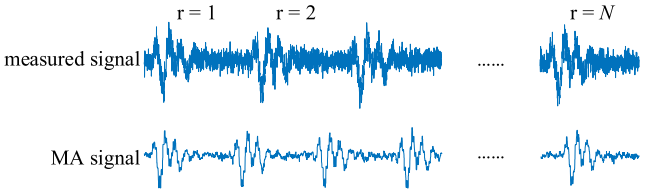

FIGURE 2. Illustration of MA algorithm.

MA is a usually used technique to reduce high frequency noises. Instead of dividing data into each cycle and averaging afterwards, MA generates the output signal by averaging several adjacent data points. For example, a MA filter with window length of 3, $y[i] = (x[i-1] + x[i] + x[i+1])/3$. Figure 2 is an illustration of MA filter. MA is good at removing random noises, especially high-frequency noises. Though MA could retain the signal length, details of the signal is lost since high frequency signal components of interest is filtered out with noise as well.

In terms of noise, there are different types of noises in engineering, including but not limited to Gaussian noises and Impulsive noises. TSA and MA mainly focus on Gaussian noises, which is also the focus of this paper. Unless otherwise specified, the noise in this paper refers to gaussian noise. Techniques to process noises of other kinds can be referred to Ref[31]–[34].

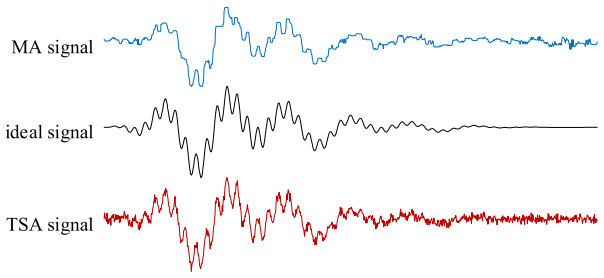

FIGURE 3. MA and TSA comparison.

Figure 3 is a comparison of MA with TSA in a cycle. Comparing TSA with ideal signal, TSA depresses signal noises effectively, and details of the signal is kept as well. However, as show in Figure 1, TSA signal contains only one cycle of the signal. TSA signal is no longer as periodic as measurement signal, moreover, spectrum resolution of the signal will degrade after processing using TSA algorithm. Comparing MA with ideal signal, MA depresses signal noises effectively as well, and the signal periodicity is retained, but details of the signal are lost though the overall trends of the signal are similar to ideal signal. MA is effective to remove

noises while keeping signal periodicity, but high frequency signal components of interests are filtered out.

Then, how to detect periodic signal among noises while keeping signal periodicity then become a challenge to TSA and MA. To address this problem, TSMA (Time Synchronous Moving Average) method is proposed in this paper. The proposed method is an improvement on TSA inspired by MA. In this way, asynchronous signal components and noise in measurement signal can be effectively depressed like TSA. At the same time, high spectrum resolution and signal periodicity can be guaranteed.

The remainder of the paper is organized as follows. Section 2 presents mathematical definition of TSMA. Influences of signal overlap and properties of TSMA are discussed in this section as well. Furthermore, a practical parameter optimization method is given for reference. Section 3 validates the theoretical deviations and effectiveness of TSMA using simulation signals. Section 4 verifies effectiveness of TSMA on periodic signal detection in engineering by applying it on fault diagnosis of gearbox. Finally, conclusions are drawn in Section 5.

II. TIME-DOMAIN SYNCHRONOUS MOVING AVERAGE AND ITS PROPERTIES

A. TIME-DOMAIN SYNCHRONOUS MOVING AVERAGE

Given periodic signal $x(t)$, and $x(t) = x(t+T)$. Measurement signal $y(t)$ contains signal $x(t)$ and noise signal $w(t)$. Noise intensity in measurement signal is D. Without losing generality, assuming N cycles signal are available for analysis. Thus

$$y(t) = x(t) + w(t),\ t \in (0, NT] \tag{1}$$

TSA signal can be expressed as following

$$\begin{aligned} y_{TSA}(t) &= \frac{1}{N}\sum\nolimits_{n=0}^{N-1} y(t+nT) \\ &= x(t) + \frac{1}{N}\sum\nolimits_{n=0}^{N-1} w(t+nT),\ t \in (0, T] \end{aligned} \tag{2}$$

Instead of averaging the signal from the beginning to the end, TSMA operates average over M neighboring cycles of the measurement signal, which is similar to that of MA. As the average window moves from the beginning to the end, $N - M + 1$ cycles of averaged signal can be obtained, rather than only 1 cycle. In this way, the TSMA signal is still periodic as measurement signal $y(t)$. Though TSMA signal contains M-1 less cycles than measurement signal $y(t)$, the TSMA signal is much longer than TSA signal. Thus, higher spectrum resolution is guaranteed.

Mathematical definition of TSMA can be written as the following:

$$\begin{aligned} y_{TSMA}(t) &= \frac{1}{M}\sum\nolimits_{m=0}^{M-1} y(t+mT) = x(t) \\ &+ \frac{1}{M}\sum\nolimits_{m=0}^{M-1} w(t+mT),\ t \in (0, (N-M+1)T] \end{aligned} \tag{3}$$

where M is the average times of TSMA. M is an integer between 1 and N.

From function (3) we can see, when $M = N$, TSMA is identical with TSA; and when $M = 1$, output of TSMA is identical to measurement signal, the measurement signal is directly outputted as it is. Another noticeable result is that noise reduction of TSMA is less effective than that of TSA since $M \leq N$.

There are two approaches to apply TSMA algorithm, namely iterative approach and convolutional approach. Iterative approach is implemented according to the definition of TSMA, the output signal is evaluated data point after data point from the beginning to the end. Convolutional approach regards TSMA as a filter, a TSMA filter is firstly constructed, it is then used to filter out noises by convoluting measurement signal and the filter.

Assuming sampled measurement signal is $y[k]$, N cycles of signal are available for analysis, and L data points are included in each cycle.

Iterative approach is carried out by the following steps:

(1) create a zero vector z that has $(N - M + 1)L$ elements.

(2) set loop variable i = 1.

(3) evaluate $z[i]$ by averaging $y[i], y[i + L], \ldots, y[i + (M - 1)L]$.

(4) i++.

(5) repeat (3) and (4) until i = $(N - M + 1)L$.

(6) outputs z.

Convolutional approach is carried out by the following steps:

(1) create a zero vector that has ML elements.

(2) set element value to $1/M$ every L elements to create a filter $\boldsymbol{f}$.

(3) convolute measurement signal with the created filter to generate output signal z.

(4) outputs z.

Figure 4 is an illustration of TSMA when $M = 3$. An interesting phenomenon of TSMA is signal overlap as the average window moves. In other words, a cycle of $y(t)$ is contained in M continuous adjacent cycles of TSMA signal. For example, 3rd cycle of measurement signal $y(t)$ is included in the average window when calculating first 3 cycles of TSMA signal. Thus, noise in M continuous adjacent cycles of TSMA signal is relevant.

Moving average strategy in TSMA promises signal periodicity and better spectrum resolution, which overcomes shortage of TSA. However, in TSMA signal, noise in adjacent cycles are relevant, and noise reduction ratio and spectrum resolution is related to average time M. Before applying TSMA in practice, several questions must be addressed first:

(1) What is the influence of signal overlap?

(2) How does spectrum resolution and gain of noise changes as M changes from 1 to N?

(3) How to determine the best M in application?

In Section 2.2, influence of signal overlap will be discussed. In Section 2.3 properties including spectrum resolution and gain of noise will be investigated. Optimization of averaging times M will be given in Section 2.4.

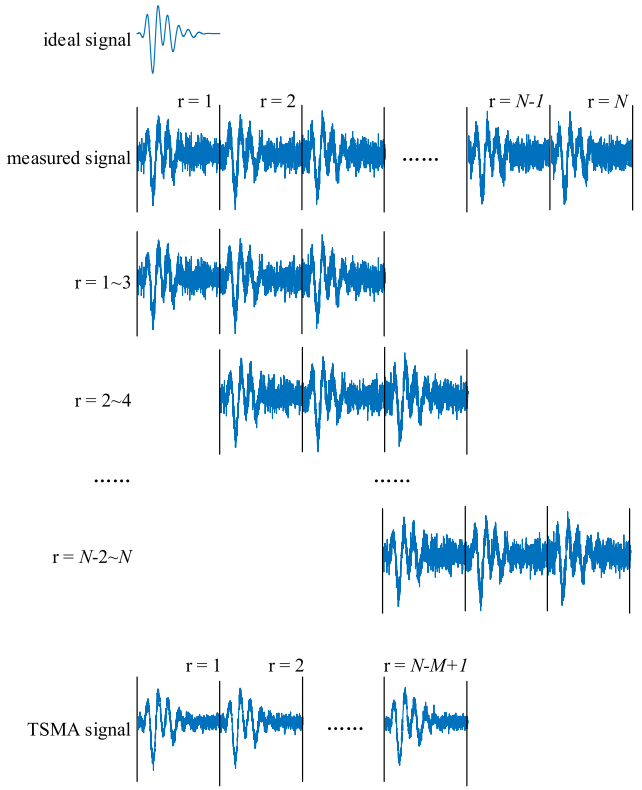

FIGURE 4. Illustration of TSMA algorithm.

B. INFLUENCE OF SIGNAL OVERLAP

1) INFLUENCE ON AUTOCORRELATION FUNCTION

For a function $x(t)$ defined on real number set, its autocorrelation function $R_x(\tau)$ is defined as

$$\begin{aligned} R_x(\tau) &= \lim_{T\to\infty}\frac{1}{T}\int_0^T x(t+\tau)x(t)dt \\ &= \lim_{T\to\infty}\frac{1}{T}\int_0^T x(t)x(t-\tau)dt \end{aligned} \tag{4}$$

In practice, signal length cannot be infinite. Autocorrelation function could be estimated using finite length signal as the following

$$\begin{aligned} \hat{R}_x(\tau) &= \frac{1}{T-\tau}\int_0^{T-\tau} x(t+\tau)x(t)dt \\ &= \lim_{T\to\infty}\frac{1}{T-\tau}\int_\tau^T x(t)x(t-\tau)dt \end{aligned} \tag{5}$$

where $\hat{R}_x(\tau)$ is the estimator of $R_x(\tau)$.

Autocorrelation function of TSA signal is

$$\hat{R}_{TSA}(\tau) = \frac{1}{T-\tau}\int_0^{T-\tau} y_{TSA}(t+\tau)y_{TSA}(t)dt = \hat{R}_x(\tau) + \frac{D}{N}\delta(\tau) \tag{6}$$

Autocorrelation function of TSMA is

$$\begin{aligned} \hat{R}_{TSMA}(\tau) &= \frac{1}{(N-M+1)T-\tau}\int_0^{(N-M+1)T-\tau} y_{TSMA}(t+\tau)y_{TSMA}(t)dt \\ &= \hat{R}_x(\tau) + \frac{D}{M^2}\sum_{k=-K}^{K} \\ &\quad \left(M - \frac{(N+1)|k|}{N-M+1} + \frac{k^2}{N-M+1}\right)\delta(\tau+kT), \\ K &= \min(N-M, M-1) \end{aligned} \tag{7}$$

Detailed deviation of function (7) is presented in Appendix A. In function (7), when $M = N$, then $K = 0$, thus

$$\begin{aligned} &\hat{R}_{TSMA}(\tau) \\ &= \hat{R}_x(\tau) + \frac{D}{M^2}\sum_{k=-0}^{0}\left(M - \frac{(N+1)|k|}{N-M+1} + \frac{k^2}{N-M+1}\right) \\ &\delta(\tau+kT) \\ &= \hat{R}_x(\tau) + \frac{D}{M^2}M\delta(\tau) \\ &= \hat{R}_x(\tau) + \frac{D}{N}\delta(\tau) \end{aligned} \tag{8}$$

Function (8) proves that, when $M = N$, TSMA is identical with TSA. This result is consistent with that in Section 2.1.

Function (7) indicates that, comparing with that of TSA signal, autocorrelation function of TSMA signal has more impulses caused by noise relevance. Amplitude of the central impulse is

$$\begin{aligned} A_k &= \frac{D}{M^2}\left(M - \frac{(N+1)|k|}{N-M+1} + \frac{k^2}{N-M+1}\right), \\ K &= \min(N-M, M-1) \end{aligned} \tag{9}$$

where A_k is impulse amplitude. When $k = 0$, the impulse is the center impulse, and its amplitude is D/M. On each side of center impulse, there are K newly appeared impulses, where $K = \min(N-M, M-1)$. These impulses spreads around central impulse with a space equals to signal period.

Summing up, influence of signal overlap on autocorrelation function includes:

(1) amplitude of central impulse caused by noise increase from D/N in TSA to D/M in TSMA.

(2) side band impulses appear around central impulse, impulses number on one side equals to min(N-M, M-1).

(3) amplitudes of newly appeared noise impulses obey a quadratic polynomial.

2) INFLUENCE ON POWER SPECTRUM

Autocorrelation function and power spectrum are Fourier Transform pairs, which can be written as:

$$G(f) = \int_{-\infty}^{+\infty} R(\tau)e^{-j2\pi f\tau}d\tau \tag{10}$$

Power spectrum of TSA signal is

$$\begin{aligned}\hat{G}_{TSA}(f) &= \int_{-\infty}^{+\infty} \hat{R}_{TSA}(\tau) e^{-j2\pi f\tau} d\tau \\ &= \int_{-\infty}^{+\infty} \left(\hat{R}_x(\tau) + \frac{D}{N}\delta(\tau)\right) e^{-j2\pi f\tau} d\tau \\ &= \hat{G}_x(f) + \frac{D}{N} \end{aligned} \tag{11}$$

Power spectrum of TSMA signal is

$$\begin{aligned}&\hat{G}_{TSMA}(f) \\ &= \int_{-\infty}^{+\infty} \hat{R}_{TSMA}(\tau) e^{-j2\pi f\tau} d\tau \\ &= \int_{-\infty}^{+\infty} \left(\hat{R}_x(\tau) + \frac{D}{M^2}\sum_{k=-K}^{K}\left(M - \frac{(N+1)|k|}{N-M+1} \right.\right. \\ &\qquad \left.\left. + \frac{k^2}{N-M+1}\right)\delta(\tau + kT)\right) e^{-j2\pi f\tau} d\tau \\ &= \hat{G}_x(f) + \frac{D}{M^2}\sum_{k=-K}^{K} \\ &\quad \left(M - \frac{(N+1)|k|}{N-M+1} + \frac{k^2}{N-M+1}\right) e^{j2\pi fkT} \\ &= \hat{G}_x(f) + \frac{D}{M} + \frac{2D}{M^2}\sum_{k=1}^{K} \\ &\quad \left(M - \frac{(N+1)k}{N-M+1} + \frac{k^2}{N-M+1}\right)\cos(2\pi fkT) \end{aligned} \tag{12}$$

Comparing power spectrum of TSA signal with TSMA signal, the influence of overlap on signal power spectrum includes:

(1) overall noise level increase from D/N in TSA to D/M in TSMA, since average times are decreased.

(2) harmonics and its multiples appears in power spectrum of TSMA signal. basic period equals to signal period. maximum order of harmonics is $K = \min(N - M, M - 1)$.

(3) amplitudes of harmonics obey a quadratic polynomial.

C. PROPERTIES OF TSMA

TSMA improves spectrum resolution of signal while keeps signal periodicity. It is noticeable that M is a parameter selected between 1 and N. How does M influence spectrum resolution and how does M influence the noise gain should be addressed for the optimal application of TSMA.

1) SPECTRUM RESOLUTION

For signal sampled with a sampling frequency of f_s, if the data points during signal collection is N_s, then spectrum resolution of the signal is

$$\Delta f = \frac{f_s}{N_s} \tag{13}$$

For a periodic signal, assuming N cycles are collected with a sampling frequency of f_s, and data points collected during each period is L. Then spectrum resolution of the measurement signal, TSA signal and TSMA signal are f_s/NL, f_s/L and $f_s/(N - M + 1)L$ respectively. Generally, Figure 5 illustrates how spectrum resolution of TSMA signal changes as M changes from 1 to N.

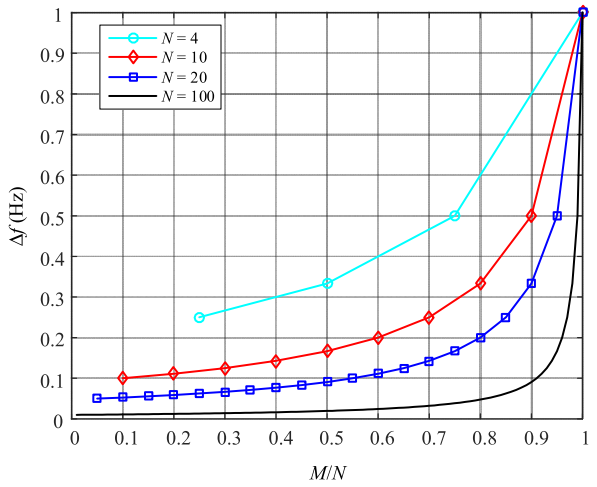

FIGURE 5. TSMA signal spectrum resolution as M changes.

From Figure 5 we can see, for a given measurement signal $y(t)$, spectrum resolution degrades as the average time increases. Moreover, when M/N is less than 0.8, spectrum resolution degrades slowly as the average time increases. Once M draws near to N, spectrum resolution degrades rapidly and converges to 1 eventually when $M = N$. Additionally, for a given average ratio M/N, spectrum resolution becomes better as N increases.

Summing up, spectrum resolution of TSMA is related to both signal cycles N and average time M. N influences the spectrum resolution on overall level, overall level of spectrum resolution will be better if signal cycles N gets larger. For a given signal, spectrum resolution degrades as M increases.

2) GAIN OF NOISE

As discussed in Section 2.2.2, power spectrum of TSMA signal is described by function (12). Background noise exist in TSMA signal power spectrum as cosine function and its harmonics, while exist as a constant number in TSA power spectrum according to function (11).

As a result, gain of noise in after applying TSMA is not intuitive as that of TSA. It is apparently unreasonable to ignore the cosine functions since they really exist. Gain of noise is defined as noise strength ratio after and before processing. According to the definition, noise within the signal will be better depressed if the gain of noise is smaller. To evaluate gain of noise after applying TSMA, the spectrum supremum of noise in TSMA signal power spectrum is regarded as the overall noise level. Thus, gain of noise could be guaranteed lower than the theoretical values.

In this way, the following inequation can be derived as the following:

$$\begin{aligned}
&\hat{G}_{TSMA}(f) \\
&= \hat{G}_x(f) + \frac{D}{M} + \frac{2D}{M^2}\sum_{k=1}^{K} \\
&\quad \left(M - \frac{(N+1)k}{N-M+1} + \frac{k^2}{N-M+1}\right)\cos(2\pi fkT) \\
&\le \hat{G}_x(f) + \frac{D}{M} + \frac{2D}{M^2}\sum_{k=1}^{K} \\
&\quad \left(M - \frac{(N+1)k}{N-M+1} + \frac{k^2}{N-M+1}\right) \\
&= \hat{G}_x(f) + \frac{D}{M} + \frac{2D}{M^2}\left(MK - \frac{(N+1)}{N-M+1}\frac{K(K+1)}{2}\right. \\
&\quad \left. + \frac{K(K+1)(2K+1)}{6(N-M+1)}\right) \qquad (14)
\end{aligned}$$

since for any $1 \le k \le K$, $\cos(2\pi fkT) = 1$ when $f = n/T$, $n = (1, 2, 3, \ldots)$.

It should be noticed that $K = \min(N - M, M\text{-}1)$. when $K = M - 1$,

$$\begin{aligned}
&\hat{G}_{TSMA}(f) \\
&\le \hat{G}_x(f) + \frac{D}{M} + \frac{2D}{M^2} \\
&\quad \times \left(MK - \frac{(N+1)}{N-M+1}\frac{K(K+1)}{2} + \frac{K(K+1)(2K+1)}{6(N-M+1)}\right) \\
&= \hat{G}_x(f) + D\frac{-4M^2+3MN+3M+1}{3M(N-M+1)} \qquad (15)
\end{aligned}$$

and when $\mathrm{K} = N - M$,

$$\begin{aligned}
&\hat{G}_{TSMA}(f) \\
&\le \hat{G}_x(f) + \frac{D}{M} + \frac{2D}{M^2} \\
&\quad \times \left(MK - \frac{(N+1)}{N-M+1}\frac{K(K+1)}{2} + \frac{K(K+1)(2K+1)}{6(N-M+1)}\right) \\
&= \hat{G}_x(f) + D\frac{-4M^2 - N^2 + 5MN - 2N + 5M}{3M^2} \qquad (16)
\end{aligned}$$

Thus, gain of noise G can be formulated as

$$G = \begin{cases} \dfrac{-4M^2+3MN+3M+1}{3M(N-M+1)} & M \le \dfrac{N+1}{2} \\ \dfrac{-4M^2-N^2+5MN-2N+5M}{3M^2} & M > \dfrac{N+1}{2} \end{cases} \qquad (17)$$

It can be proved from function (15) that gain of noise decreases as average time M increases, which means noise will be depressed stronger as M increases. when $M = N$, $G = 1/N$, gain of noise after applying TSMA equals to that of TSA.

Figure 6 shows how gain of noise changes as M/N changes.

It must be emphasized that noise gain discussed in this subsection is NOT the mean noise gain over the frequency axis in power spectrum, but the supremum of back ground noise power spectrum distribution. When applying TSMA, the noise gain will be less than theoretical values evaluated using function (15).

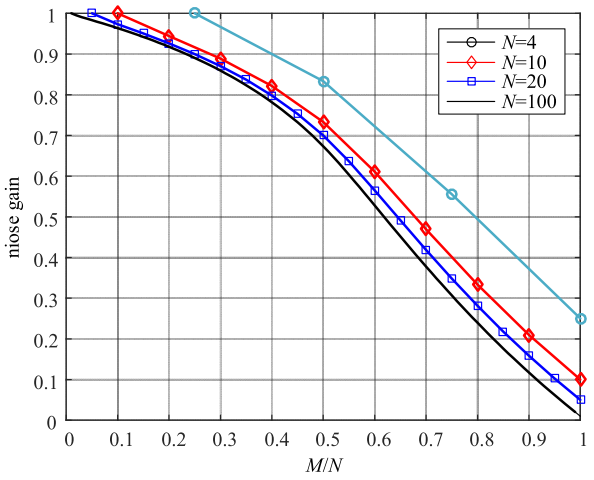

FIGURE 6. TSMA noise gain as M changes.

D. AVERAGE TIME M OPTIMIZATION

From Section 2.3 we can see, it needs to balance between spectrum resolution and gain of noise when applying TSMA. If a small average time M is selected, better spectrum resolution is guaranteed but noise is not effectively depressed. On the contrast, noise is depressed remarkably but spectrum resolution degrades when large average time M is selected.

Without an optimization criterion, the chosen of M is subjective to the one who is using TSMA. One may expect better gain of noise while others are interested in better spectrum resolution. From the perspective of the authors, M choosing between $0.5N$ and $0.9N$ is more reasonable than others. Others may not agree with this idea. Thus, a method for M optimization is needed to guide the application of TSMA.

Practically, an optimization object function for M optimization is proposed as the following

$$O[M] = \Delta f + G \qquad (18)$$

Shown in figure 7 is how $O[M]$ changes as M/N changes. Taking $N = 10$ for example, figure 7 suggests that the best M/N is 0.8, then $M = 8$ can be used to balance between noise gain and spectrum resolution when using TSMA.

It should be noticed that the average time optimization is just one of the optimization methods to balance between spectrum resolution and noise gain. Users are encouraged to develop other methods suitable for specific applications.

III. SIMULATION VALIDATION

To validate the theoretical deviations above, simulation signals are generated and analyzed, the proposed TSMA method is compared with TSA.

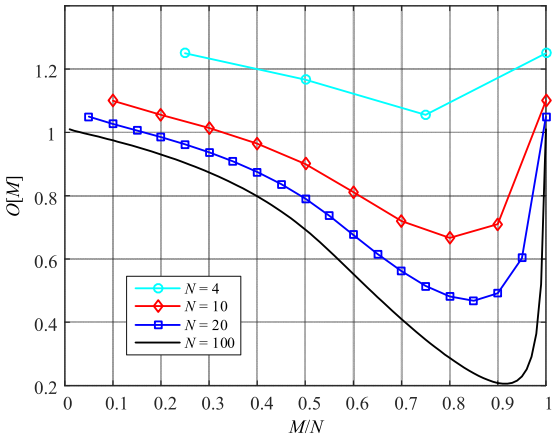

FIGURE 7. *O*[*M*] as *M* changes.

A. THEORETICAL DEVIATIONS VALIDATION USING GAUSSIAN NOISE

To investigate theoretical deviations of TSMA in Section 2, no deterministic signal is included in first simulation. Sampling rate of simulation signal is 1024, detection period T is 0.5 seconds. Signal length is 5s, which covers 10 detection periods. Power of noise is set as 100W. Average times of TSMA is set as 8 according to the optimization criterion.

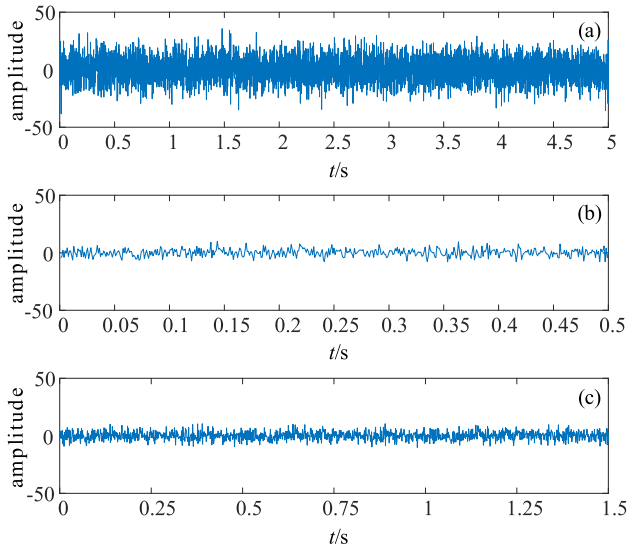

FIGURE 8. Waveform of signal (a) simulation signal (b) TSA signal (c) TSMA signal.

Waveform of simulation signal, TSA signal and TSMA signal are shown in figure 8. Comparing with simulation signal, both TSA and TSMA can depress noise significantly. Noise strength is depressed to the same level in TSA and TSMA signal. However, TSMA signal is obviously longer than TSA signal, which promises a better spectrum resolution.

Shown in Figure 9 is autocorrelation of simulation signal, TSA signal and TSMA signal. Comparing with simulation signal, central impulse amplitude in autocorrelation of TSA

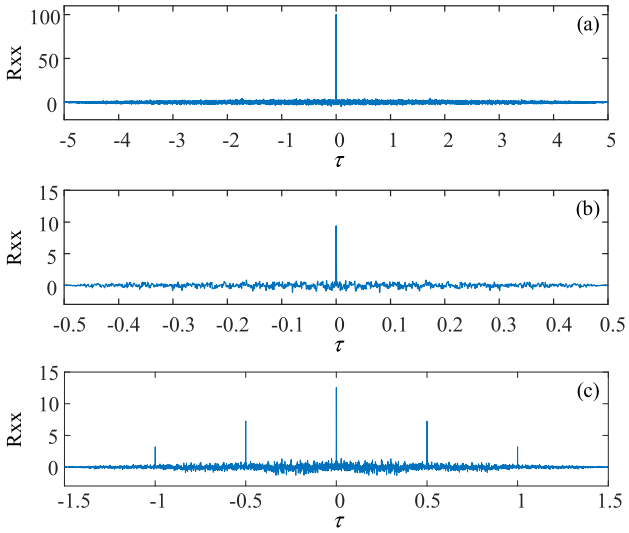

FIGURE 9. Autocorrelation of signal (a) simulation signal (b) TSA signal (c) TSMA signal.

and TSMA are depressed effectively from 100 to around 10. This phenomenon indicates that both TSA and TSMA are good at depressing overall noise level using average techniques. In addition, central impulse amplitude in autocorrelation function of TSMA signal is a little larger than that of TSA because average times in TSMA is less than that in TSA. It is also nonnegligible that fading impulses emerge around central impulse in autocorrelation of TSMA, which is caused by signal overlap during moving average. Number of impulses on one side, either left or right, is 2, which equals to $K = \min(N - M, M - 1)$.

Figure 10 is expected and observed amplitudes of impulses in TSMA signal autocorrelation function. Expected amplitudes are evaluated according to function (7) while observed amplitudes are measured from Figure 9(c). Figure 10 indicates that the observed amplitudes are consistent with expected values.

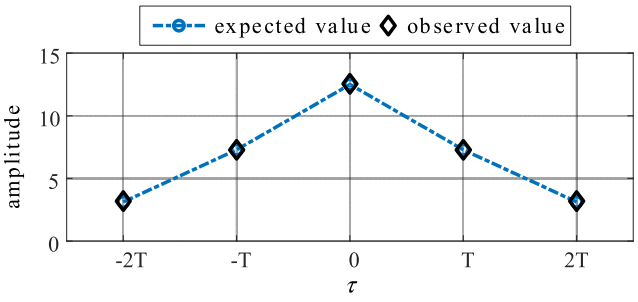

FIGURE 10. Impulses amplitudes in TSMA autocorrelation.

Autocorrelation function analysis indicates that related theoretical deviations in Section 2.2.1 is correct.

Figure 11 is power spectrums of simulation signal, TSA signal and TSMA signal respectively. Theoretical noise gain of TSMA is illustrated in the figure as well.

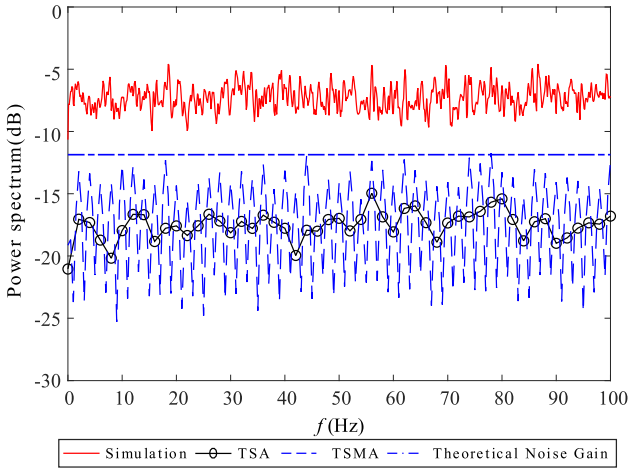

FIGURE 11. Power spectrums of simulation signal.

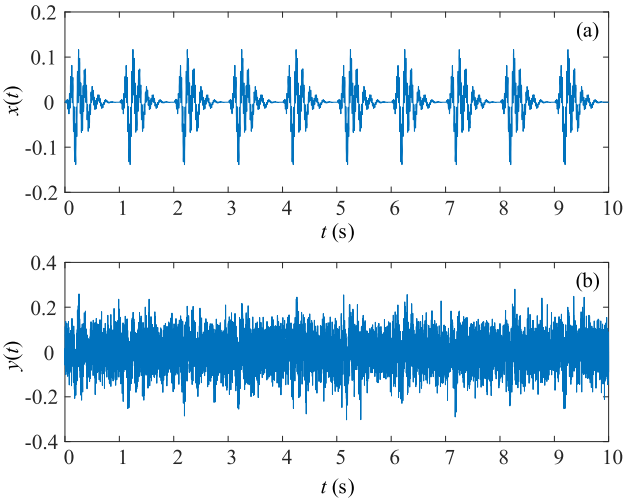

FIGURE 12. Waveform of simulation signal (a) ideal signal $x(t)$ (b) measurement signal y(t).

In Section 2.3.2, supremum of power spectrum is regarded as the overall noise gain since PSD of noise appears in PSD of TSMA signal as cosine wave and its harmonics. As shown in the figure, theoretical noise gain of TSMA is the supremum of TSMA PSD, which indicates that theoretical deviation in Section 2.3.2 is correct. Comparing noise gain of TSA with that of TSMA, both TSA and TSMA can depress noise level effectively. However, noise gain of TSA is smaller than that of TSMA since averaging times is larger.

Summing up, simulation analysis using pure gaussian noise signal proves that theoretical deviations in Section 2 is correct and reliable.

B. EFFECTIVENESS VALIDATION AND COMPARISON

In this section, simulation signal is generated and used to validate effectiveness of TSMA on periodic signal detection. Sampling rate of simulation signal is 1024, detection period T is 1 seconds, signal length is 10s, which covers 10 detection periods. SNR of simulation signal is -6.15 dB.

Figure 12 is waveform of simulation signal, which is periodic transient impulses overwhelmed by heavy noise. Shown in Figure 12(a) is the ideal signal waveform. It is periodic transient signal. Shown in Figure 12(b) is the measurement signal that is polluted by the heavy noise. No evident periodicity can be observed from the measurement signal waveform, neither pattern or shape of transient impulses.

Then, the simulation signal is processed using TSA, MA and TSMA respectively. Shown in Figure 13 is TSA signal, TSMA signal and MA signal.

Figure 13 highly suggests that TSA, TSMA and MA are all effective to detect periodic signal among noise. Comparing TSA with TSMA, Noise in TSMA is a little stronger than that in TSA signal. This is reasonable since TSA depresses the noise more efficiently. However, TSA signal covers only 1 cycle of the signal while TSMA contains 4 cycles. TSA is capable of detecting signal waveform, but the period of the signal is lost. Comparing TSMA with MA, both TSMA

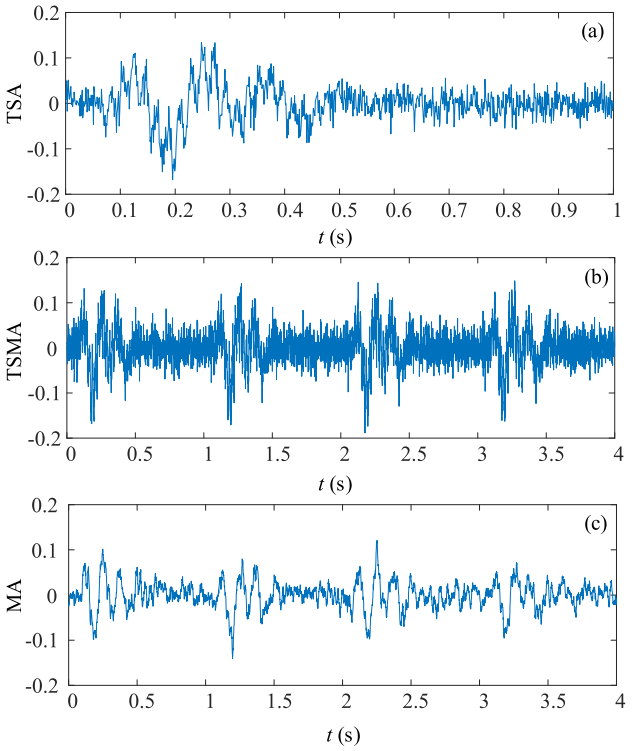

FIGURE 13. Processing result (a) TSA (b) TSMA (c) MA.

and MA maintains signal periodicity, which is better than TSA. Signal waveform indicates that MA depresses the noise more effective than TSMA. However, waveform details in Figure 13(c) differs from the ideal. Though signal periodicity is maintained, but signal details are lost in MA.

For a better comparison on signal waveform details. Ideal signal, TSMA signal, TSA signal and MA signal in a cycle are presented in Figure 14. Figure 14(a) is the waveform of ideal signal. Waveform of TSMA, TSA and MA are shown in Figure 14 (b), (c) and (d) respectively. Comparing 14(b)

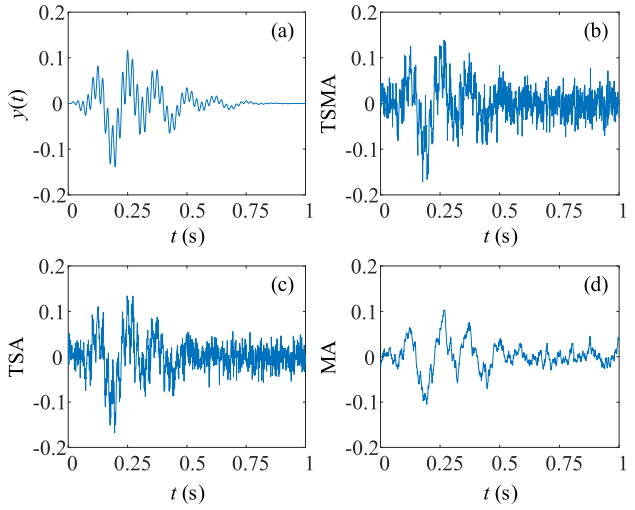

FIGURE 14. Signal waveform in a cycle (a) ideal (b) TSMA (c) TSA (d) MA.

with 14(c), TSMA signal waveform is similar to TSA signal, the difference is strength of the noise since TSA depress noise more effective than TSMA. Comparing 14(b) with 14(d), MA signal waveforms contains less noise. However, MA waveforms differs a lot from the ideal signal, especially high frequency details.

Spectrum of ideal signal, TSMA, TSA and MA are shown in Figure 15.

Comparing Figure 15(a) with 15(b), spectrum of TSMA is close to that of ideal signal, frequency peaks are almost kept. Spectrum of TSMA differs from that of ideal signal from two aspects: (1) spectrum resolution of TSMA is not as good as the ideal signal, but it's still able to distinguish frequency components of the signal. (2) background noise exists in the spectrum, but the noise does not interfere distinguishing frequency components.

Comparing Figure 15(a) with 15(c), spectrum structure of TSA is same with ideal signal, but only several frequencies could be observed since spectrum resolution degrades seriously. Comparing Figure 15(b) and 15(c), the dominant difference is also spectrum resolution. As a result, TSMA can distinguish all frequency components within ideal signal while TSA cannot.

Comparing Figure 15(a) with 15(d), spectrum resolution of MA is almost same as that of ideal signal since frequency components below 10 Hz can be easily observed. However, frequency components between 45 and 55 Hz are filtered out since MA works as a low-pass filter. Therefore, details of signal waveform are lost after processing using MA. Comparing Figure 15(b) with 15(d), the dominant difference is also frequency components between 45 and 55 Hz. TSMA keeps high frequency component, which helps to guarantee signal waveform details.

Additionally, *SNR* of TSA signal is 3.89 dB, *SNR* of TSMA signal is 2.31 dB, *SNR* of MA signal is 3.64dB. From *SNR* value we can see that TSA, TSMA and MA all improves *SNR*

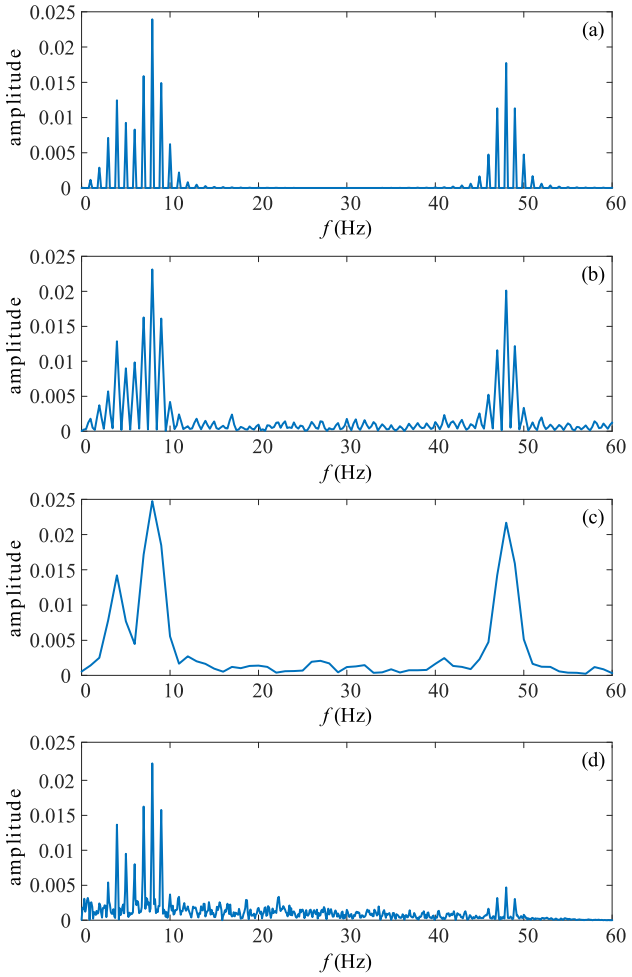

FIGURE 15. Spectrum comparison (a) ideal (b) TSMA (c) TSA (d) MA.

effectively. Though *SNR* of TSMA is a little worse than that of TSA, spectrum resolution of TSMA is much better. Spectrum resolution of TSA is 1 while that of TSMA is 0.25. Though *SNR* of TSMA is a little worse than that of MA, TSMA can maintain signal waveform details while MA cannot.

Simulation of periodic transient signal detection indicates that TSMA can effectively detect periodic signal that overwhelmed by noise. Moreover, spectrum resolution of TSMA improves dramatically comparing with TSA, additionally, high frequency components are kept guaranteeing signal waveform details comparing with MA.

IV. APPLICATION OF TSMA ON FAULT DETECTION OF GEARBOX

In order to demonstrate ability of TSMA algorithm on periodic signal detection in practice, an experimental case study was conducted to collect gearbox vibration signals for fault detection purposes.

When gearbox is under health condition, vibrations of gearbox mainly includes regular signal components such as shaft rotating frequency, gear meshing frequency and their harmonics. Once a gear tooth is damaged during operation,

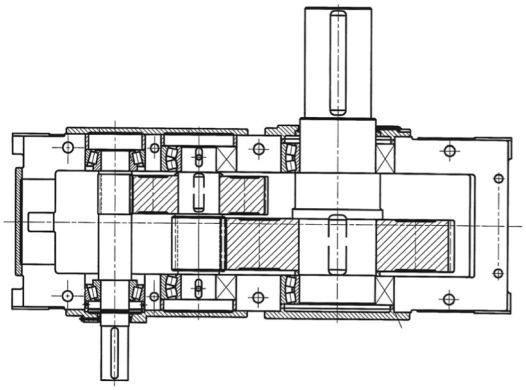

FIGURE 16. Assembly drawing of the gearbox.

damaged gear will change the meshing stiffness when it's engaged in meshing. The vibration responses of gearbox will change accordingly when the damaged gear tooth meshes out. Gear fault induced vibrations appears in the overall vibration responses of gearbox as sequent impulses. Since the damaged gear tooth engages in meshing once per revolution, detection of periodic impulses signal is a practical method for gearbox fault detection.

In this section, TSMA is used as a signal processing technique to diagnose gear fault in a gearbox. The gearbox is a 2-stage fixed-shaft gearbox. Assembly drawing of the gearbox is shown in Figure 16.

Parameters of the gearbox is listed in Table 1.

TABLE 1. Gearbox parameters.

Stage	Gear tooth number	Transmission ratio
1	21	4.38
	92	
2	18	4.88
	88	

During each test, motor speed is set as 1500 rpm, torque of load motor is 80% of maximum load. Sampling rate is 12707Hz.

Figure 17 is picture of faulted gear. The fault is a pitting emerged during operation. After replaced by a normal gear, this faulted gear is then used for pitting fault detection and diagnosis studies.

Figure 18 shows vibration signals of gearbox under health and fault condition respectively. Due to regular vibrations caused by time varying meshing stiffness and noise, fault related impulses could hardly be observed in time domain waveforms directly.

The vibration signals of gearbox are then processed using TSA, TSMA and MA. Signal processing results are illustrated in Figure 19 and Figure 20. For better comparison, signal envelops are outlined as well. TSA, TSMA and MA envelop spectrum are shown in Figure 21.

FIGURE 17. Gear with pitting fault.

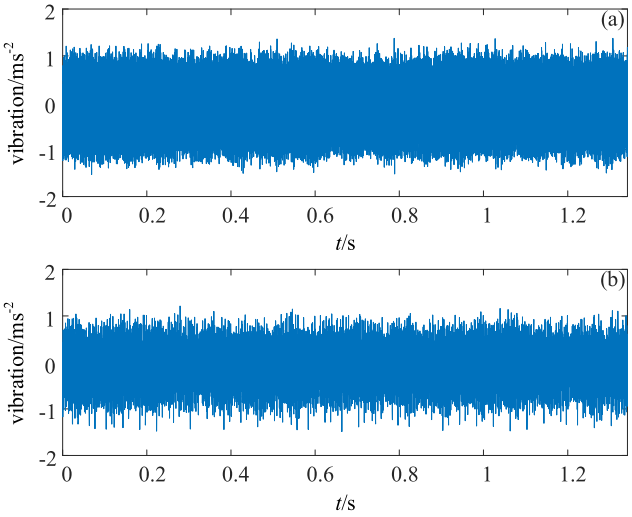

FIGURE 18. Vibration signal (a) health condition (b) fault condition.

Firstly, Comparison of TSMA signal between under health condition and fault condition is made to validate effectiveness of TSMA on gearbox fault detection. Figure 19(c) is TSMA signal under health condition, while Figure 20(c) is TSMA signal under fault condition. Under health condition, TSMA algorithm depress signal noise apparently, signal amplitude is decreased from 1 to around 0.2. No apparent impulsive signal components can be observed. When the gear tooth is damaged by pitting, impulsive signal emerges in TSMA signal as shown in Figure 20(c). Impulses appear once in a gear revolution, which is consistent with gearbox fault symptom. Comparison of TSMA signal between under health condition and fault condition indicates that TSMA is effective to detect gearbox fault.

Envelop spectrum of TSMA signal under health condition and fault condition reveals effectiveness of TSMA as well. Comparing solid lines in Figure 21(a) with 21(b), amplitude of envelop spectrum at 1st, 2nd and 3rd order increase significantly from around 0.01 to 0.02 and above.

Secondly, Comparison is made to demonstrate advantage and disadvantage of TSMA relative to TSA and MA.

In terms of noise depression, comparison is made under health and fault condition respectively. Comparing Figure 19(a) with 19(b), TSA and TSMA depress the noise

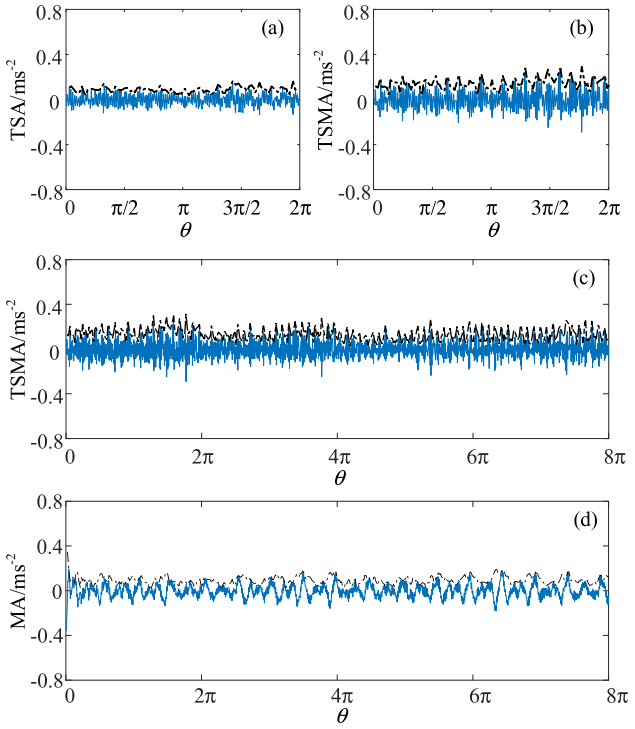

FIGURE 19. Processing results under health condition (a) TSA (b) 1st cycle of TSMA (c) TSMA (d) MA.

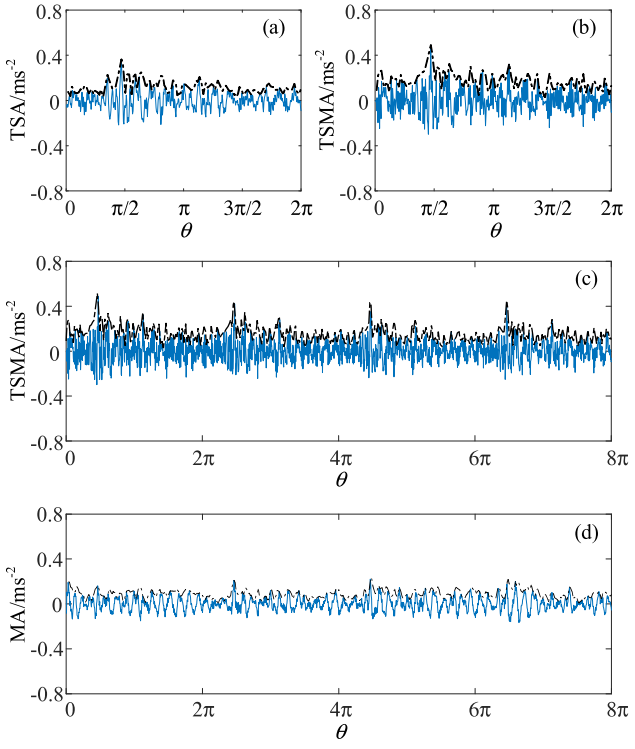

FIGURE 20. Processing results under fault condition (a)TSA (b) 1st cycle of TSMA (c)TSMA (d) MA.

to almost the same level, but signal amplitude of TSMA is a little higher than TSA. The same situation can be found when comparing Figure 20(a) with 20(b). This result is consistent with theoretical deviations and simulation validation on signal detection since moving average times of TSMA is less than that of TSA. Comparing Figure 19(c) and 19(d), MA depresses the noise more effectively, especially high frequency noise. This can also be seen by comparing Figure 20(c) with 20(d). However, fault induced impulses could be easily observed in TSA and TSMA signal while not in MA signal. Fault induced impulses are depressed in MA since high frequency signal components are filtered out.

In terms of effectiveness on fault detection of gearbox, comparison is made between health condition and fault condition. Comparing Figure 19 (a) with Figure 20(a), Figure 19(b) with Figure 20(b), both TSA and TSMA is effective to detect the fault induced impulsive signal. However, TSMA signal is much longer than TSA signal (in Figure19(c) and Figure 20(c)). The fault induced impulses appear periodically in TSMA but only once in TSA. Period of the impulses helps to ensure the impulsive signal detected is fault related. Comparing Figure 19(d) with Figure 20(d), fault induced impulses could be hardly observed since high frequency components are filtered out by MA.

Signal envelop spectrum under health and fault condition are shown in Figure 21.

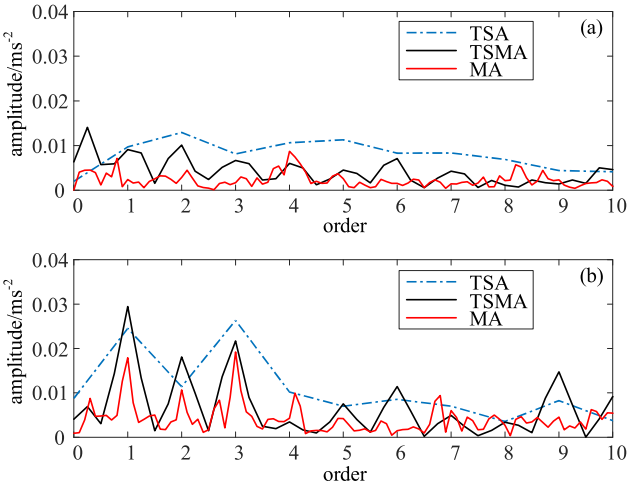

FIGURE 21. Envelop spectrum of TSA, TSMA and MA (a) health condition (b) fault condition.

First, comparison is made focusing on spectrum resolution. A comparison between Figure 21(a) with 21(b) indicates that TSMA keeps more frequency details than TSA since better spectrum resolution is guaranteed. In Figure 21(b), 2nd order of TSA envelop spectrum is not noticeable but it can be easily seen in TSMA envelop spectrum. Spectrum resolution of MA is the best since MA causes no spectrum resolution degradation.

Then, comparison is made focusing on effectiveness on fault detection. Differences between Figure 21(a) and 21(b) suggests that TSA, TSMA and MA are all effective to detect gearbox fault since pattern of spectrum changes when fault occurs. However, MA and TSMA are better than TSA

since better spectrum resolution provides more spectrum details, spectrum differences caused by gear damage is more apparent.

It may be hard to tell MA or TSMA is better from the spectrum, but fault induced impulses could be easier recognized from waveform of TSMA.

Experimental results indicate that:

(1) TSMA is as effective as TSA and MA on fault detection of gearbox. When gear fault happens, fault induced impulses could be effectively detected.

(2) Fault induced impulses appear periodically in TSMA. Period of the impulses helps to ensure the impulsive signal detected is fault related.

(3) TSA has better gain of noise, but TSMA keeps more detail in frequency domain since better spectrum resolution is guaranteed.

(4) MA has better gain of noise as well, spectrum resolution is also as good as TSMA, but TSMA keeps signal high frequency components, which helps recognizing fault induced impulses from signal waveform.

V. CONCLUSION

TSA and MA are most often used averaging techniques in periodic signal detection. TSA could depress noise and keep details of the periodic signal, but it covers only 1 cycle of the signal. Accordingly, spectrum resolution degrades seriously. MA keeps the signal length, but losing details of the signal. TSMA is proposed to combine the advantage of TSA and MA. After given mathematical definition of TSMA, influence of signal overlap and properties of TSMA are discussed theoretically, as well as a practical method to determine the best average times to balance noise gain and spectrum resolution. The correctness of theoretical deviations is validated using numerical simulation. Effectiveness of TSMA on periodic signal detection is demonstrated using both simulation and experiment. Results of simulation and experiment indicate that TSMA could detect periodic signal successfully while guaranteeing spectrum resolution.

APPENDIX DETAILED DEVIATION OF FUNCTION (7)

Autocorrelation function of TSMA signal is

$$\begin{aligned}\hat{R}_{TSMA}(\tau) &= \frac{1}{(N-M+1)T-\tau} \times \int_0^{(N-M+1)T-\tau} y_{TSMA}(t+\tau)y_{TSMA}(t)dt \\ &= \frac{1}{(N-M+1)T-\tau}\int_0^{(N-M)T-\tau} \left[x(t+\tau)+\frac{1}{M}\sum_{n=0}^{M-1} w(t+\tau+nT)\right] \times \left[x(t)+\frac{1}{M}\sum_{j=0}^{M-1} w(t+jT)\right] dt \\ &= \hat{R}_x(\tau)+\frac{1}{M^2}\sum_{j=0}^{M-1}\sum_{n=0}^{M-1}\frac{1}{(N-M+1)T-\tau} \times \int_0^{(N-M+1)T-\tau} w(t+jT)w(t+\tau+nT)dt \end{aligned} \tag{A.1}$$

Taking advantage of Heaviside step function, function (A.1) can be written as

$$\begin{aligned}\hat{R}_{TSMA}(\tau) &= \hat{R}_x(\tau)+\frac{D}{M^2}\sum_{j=0}^{M-1}\sum_{n=0}^{M-1} H\left[(N-M+1)-|n-j|\right] \times \frac{(N-M+1)-|n-j|}{(N-M+1)}\delta\left(\tau+(n-j)T\right) \end{aligned} \tag{A.2}$$

where $H[n]$ is Heaviside step function. It is defined as

$$H[n]=\begin{cases}0, & n<0\\ 1, & n\geq 0\end{cases} \tag{A.3}$$

Let $Q=N-M+1, k=n-j$. Function (A.2) can be written as

$$\hat{R}_{TSMA}(\tau)=\hat{R}_x(\tau)+\frac{D}{M^2}\sum_{k=-(M-1)}^{M-1} H[Q-|k|] \times \frac{(Q-|k|)(M-|k|)}{Q}\delta(\tau+kT) \tag{A.4}$$

when $Q\geq M-1$, namely when $M\leq (N+2)/2$, $H[Q-|k|]==1$ since $|k|\leq M-1\leq Q$, thus

$$\begin{aligned}\hat{R}_{TSMA}(\tau) &= \hat{R}_x(\tau)+\frac{D}{M^2}\sum_{k=-(M-1)}^{M-1} H[Q-|k|] \times \frac{(Q-|k|)(M-|k|)}{Q}\delta(\tau+kT) \\ &= \hat{R}_x(\tau)+\frac{D}{M^2}\sum_{k=-(M-1)}^{M-1} \frac{(Q-|k|)(M-|k|)}{Q}\delta(\tau+kT) \\ &= \hat{R}_x(\tau)+\frac{D}{M^2}\sum_{k=-(M-1)}^{M-1} \frac{QM-(Q+M)|k|+k^2}{Q}\delta(\tau+kT) \\ &= \hat{R}_x(\tau)+\frac{D}{M^2}\sum_{k=-(M-1)}^{M-1} \left(M-\frac{(Q+M)|k|}{Q}+\frac{k^2}{Q}\right)\delta(\tau+kT) \end{aligned} \tag{A.5}$$

On the contrast, when $Q\leq M-1$, namely when $M\leq (N+2)/2$, $H[Q-|k|]=0$ if $|k|\geq Q$, thus

$$\hat{R}_{TSMA}(\tau)=\hat{R}_x(\tau)+\frac{D}{M^2}\sum_{k=-(M-1)}^{M-1} H[Q-|k|] \times \frac{(Q-|k|)(M-|k|)}{Q}\delta(\tau+kT)$$

$$= \hat{R}_x(\tau) + \frac{D}{M^2} \sum_{k=-Q}^{Q} \frac{(Q-|k|)(M-|k|)}{Q} \delta(\tau + kT)$$

$$= \hat{R}_x(\tau) + \frac{D}{M^2} \sum_{k=-(Q-1)}^{Q-1} \frac{QM - (Q+M)|k| + k^2}{Q} \delta(\tau + kT)$$

$$= \hat{R}_x(\tau) + \frac{D}{M^2} \sum_{k=-(Q-1)}^{Q-1} \left(M - \frac{(Q+M)|k|}{Q} + \frac{k^2}{Q} \right) \delta(\tau + kT) \tag{A.6}$$

Summing up,

$$\hat{R}_{TSMA}(\tau) = \hat{R}_x(\tau) + \frac{D}{M^2} \sum_{k=-K}^{K} \left(M - \frac{(N+1)|k|}{N-M+1} + \frac{k^2}{N-M+1} \right) \delta(\tau + kT), \quad K = \min(N-M, M-1) \tag{A.7}$$

ACKNOWLEDGMENT

The author would like to express his very great appreciation to Professor Fengshou Gu from University of Huddersfield for his valuable suggestions, patient guidance and enthusiastic encouragement during the development of this research work. His willingness to give his time so generously has been very much appreciated.

REFERENCES

[1] H. Baali, R. Akmeliawati, M. J. E. Salami, M. Aibinu, and A. Gani, "Transform based approach for ECG period normalization," in *Proc. Comput. Cardiol.*, Sep. 2011, pp. 533–536.

[2] Z. Yu, W. Hao, and C. Yong, "Period estimation of PN sequence for weak DSSS signals based on improved power spectrum reprocessing in non-cooperative communication systems," in *Proc. Int. Conf. Control Eng. Commun. Technol.*, Dec. 2012, pp. 924–927.

[3] R. A. Lara-Cueva, D. S. Benítez, E. V. Carrera, M. Ruiz, and J. L. Rojo-Álvarez, "Automatic recognition of long period events from volcano tectonic earthquakes at cotopaxi volcano," *IEEE Trans. Geosci. Remote Sens.*, vol. 54, no. 9, pp. 5247–5257, Sep. 2016.

[4] S. Jain and H. Hunt, "Vibration response of a wind-turbine planetary gear set in the presence of a localized planet bearing defect," in *Proc. Int. Mech. Eng. Congr. Expo.*, Nov. 2011, pp. 943–952.

[5] A. Simm, Q. Wang, S. Huang, and W. Zhao, "Laser based measurement for the monitoring of shaft misalignment," *Measurement*, vol. 87, pp. 104–116, Jun. 2016.

[6] Z. Cheng, "A hybrid prognostics approach to estimate the residual useful life of a planetary gearbox with a local defect," *J. Vibroeng.*, vol. 17, no. 2, pp. 682–694, Mar. 2015.

[7] R. Ahmed, M. El Sayed, S. A. Gadsden, J. Tjong, and S. Habibi, "Automotive internal-combustion-engine fault detection and classification using artificial neural network techniques," *IEEE Trans. Veh. Technol.*, vol. 64, no. 1, pp. 21–33, Jan. 2015.

[8] J. Li, Z. Zeng, J. Sun, and F. Liu, "Through-wall detection of human being's movement by UWB radar," *IEEE Geosci. Remote Sens. Lett.*, vol. 9, no. 6, pp. 1079–1083, Nov. 2012.

[9] M. Sekine and K. Maeno, "Non-contact heart rate detection using periodic variation in Doppler frequency," in *Proc. IEEE Sensors Appl. Symp.*, Feb. 2011, pp. 318–322.

[10] H. Choi, A. V. Gomes, and A. Chatterjee, "Signal acquisition of high-speed periodic signals using incoherent sub-sampling and back-end signal reconstruction algorithms," *IEEE Trans. Very Large Scale Integr. (VLSI) Syst.*, vol. 19, no. 7, pp. 1125–1135, Jul. 2011.

[11] W. R. Leeb, A. Poppe, E. Hammel, J. Alves, M. Brunner, and S. Meingast, "Single-photon technique for the detection of periodic extraterrestrial laser pulses," *Astrobiology*, vol. 13, no. 6, pp. 35–521, Jun. 2013.

[12] Z.-D. Tsai and M.-H. Perng, "Defect detection in periodic patterns using a multi-band-pass filter," *Mach. Vis. Appl.*, vol. 24, no. 3, pp. 551–565, 2013.

[13] X. Xu, M. Zhao, J. Lin, and Y. Lei, "Envelope harmonic-to-noise ratio for periodic impulses detection and its application to bearing diagnosis," *Measurement*, vol. 91, pp. 385–397, Sep. 2016.

[14] Y. Yao and J. Ma, "Weak periodic signal detection by sine-Wiener-noise-induced resonance in the FitzHugh–Nagumo neuron," *Cogn. Neurodyn.*, vol. 12, no. 3, pp. 343–349, Jun. 2018.

[15] E. Yilmaz and M. Ozer, "Delayed feedback and detection of weak periodic signals in a stochastic Hodgkin–Huxley neuron," *Phys. A, Stat. Mech. Appl.*, vol. 421, pp. 455–462, Mar. 2015.

[16] P. McFadden and J. D. Smith, "A signal processing technique for detecting local defects in a gear from the signal average of the vibration," *Proc. Inst. Mech. Eng. C, J. Mech. Eng. Sci.*, vol. 199, no. 4, pp. 287–292, Feb. 1985.

[17] P. D. McFadden and M. M. Toozhy, "Application of synchronous averaging to vibration monitoring of rolling element bearings," *Mech. Syst. Signal Process.*, vol. 14, no. 6, pp. 891–906, Nov. 2000.

[18] P. D. McFadden, "A technique for calculating the time domain averages of the vibration of the individual planet gears and the sun gear in an epicyclic gearbox," *J. Sound Vib.*, vol. 144, no. 1, pp. 163–172, Jan. 1991.

[19] Q. Leclère and N. Hamzaoui, "Using the moving synchronous average to analyze fuzzy cyclostationary signals," *Mech. Syst. Signal Process.*, vol. 44, pp. 149–159, Feb. 2014.

[20] Y. Guo, X. Wu, J. Na, and R.-F. Fung, "Envelope synchronous average scheme for multi-axis gear faults detection," *J. Sound Vib.*, vol. 365, pp. 276–286, Mar. 2016.

[21] E. Bechhoefer and M. Kingsley, "A review of time synchronous average algorithms," in *Proc. Annu. Conf. Prognostics Health Manage. Soc.*, vol. 1, Sep. 2009, pp. 1–10.

[22] N. Ahamed, Y. Pandya, and A. Parey, "Spur gear tooth root crack detection using time synchronous averaging under fluctuating speed," *Measurement*, vol. 52, pp. 1–11, Jun. 2014.

[23] I. Bravo-Imaz, H. D. Ardakani, Z. Liu, A. Garcia-Arribas, A. Arnaiz, and J. Lee, "Motor current signature analysis for gearbox condition monitoring under transient speeds using wavelet analysis and dual-level time synchronous averaging," *Mech. Syst. Signal Process.*, vol. 94, pp. 73–84, Sep. 2017.

[24] F. Combet and L. Gelman, "An automated methodology for performing time synchronous averaging of a gearbox signal without speed sensor," *Mech. Syst. Signal Process.*, vol. 21, no. 6, pp. 2590–2606, Aug. 2007.

[25] J. M. Ha, B. D. Youn, H. Oh, B. Han, Y. Jung, and J. Park, "Autocorrelation-based time synchronous averaging for condition monitoring of planetary gearboxes in wind turbines," *Mech. Syst. Signal Process.*, vols. 70–71, pp. 161–175, Mar. 2016.

[26] L. Zhu, H. Ding, and X. Y. Zhu, "Synchronous averaging of time-frequency distribution with application to machine condition monitoring," *J. Vib. Acoust.*, vol. 129, no. 4, pp. 441–447, Mar. 2007.

[27] Y. Qin, J. Zou, B. Tang, Y. Wang, and H. Chen, "Transient feature extraction by the improved orthogonal matching pursuit and K-SVD algorithm with adaptive transient dictionary," *IEEE Trans. Ind. Informat.*, to be published.

[28] S. Braun, "The synchronous (time domain) average revisited," *Mech. Syst. Signal Process*, vol. 25, no. 4, pp. 1087–1102, May 2011.

[29] S. W. Smith, "Moving average filters," in *The Scientist and Engineer's Guide to Digital Signal Processing*. Lompoc, CA, USA: California Technical Publication, 1991, pp. 277–284.

[30] A. A. Hood, "Fault detection on a full-scale OH-58 A/C helicopter transmission," Ph.D. dissertation, Univ. Maryland, College Park, MD, USA, 2010.

[31] W. Biao, F. Yu, W. Yang, and C. He, "An adaptive data detection algorithm based on intermittent chaos with strong noise background," in *Neural Computing and Applications*. London, U.K.: Springer, 2018, pp. 1–8.

[32] F. Chen, T. Shi, S. Duan, L. Wang, and J. Wu, "Diffusion least logarithmic absolute difference algorithm for distributed estimation," *Signal Process.*, vol. 142, pp. 423–430, Jan. 2018.

[33] F. Chen, X. Li, S. Duan, L. Wang, and J. Wu, "Diffusion generalized maximum correntropy criterion algorithm for distributed estimation over multitask network," *Digit. Signal Process.*, vol. 81, pp. 16–25, Oct. 2018.

[34] F. Chen and X. Shao, "Broken-motifs diffusion LMS algorithm for reducing communication load," *Signal Process.*, vol. 133, pp. 213–218, Apr. 2017.

LUN ZHANG received the B.S. and M.S. degrees in mechanical engineering from the National University of Defense Technology, in 2013 and 2015, respectively. He is currently pursuing the Ph.D. degree in mechanical engineering with the University of Defense Technology. His research interests include dynamic modeling, signal processing, and machinery fault diagnosis.

NIAOQING HU received the B.S., M.S., and Ph.D. degrees in mechanical engineering from the National University of Defense Technology, in 1989, 1992, and 2001, respectively.

From 1993 to 1998, he was a Lecturer with the Department of Mechanical and Electronic Engineering and Instrumentation. From 1998 to 2003, he was an Associate Professor with the Department of Mechatronics and Automation. Since 2004, he has been a Professor with the National University of Defense Technology. He is the author of four books, over 260 articles, and more than seven inventions. His research interests include condition monitoring, prognosis and health management, signal processing, mechanical dynamics, nonlinear systems, structure health monitoring, and artificial intelligence.